DOE/ET/53088--697

INSTITUTE FOR FUSION STUDIES

DE-FG05-80ET-53088-697 IFSR #697

Shear Flow Effects on Ion Thermal Transport in Tokamaks

T. TAJIMA, Y. KISHIMOTO,[a] W. HORTON, and J.Q. DONG
Institute for Fusion Studies
The University of Texas at Austin
Austin, Texas 78712

March 1995

[a] Naka Fusion Research, JAERI, Japan

THE UNIVERSITY OF TEXAS

AUSTIN

DISCLAIMER

DISCLAIMER

Portions of this document may be illegible in electronic image products. Images are produced from the best available original document.

Shear flow effects on ion thermal transport in tokamaks

T. Tajima,* Y. Kishimoto,[a] W. Horton, and J.Q. Dong
Institute for Fusion Studies, The University of Texas at Austin
Austin, Texas 78712

Abstract

From various laboratory and numerical experiments, there is clear evidence that under certain conditions the presence of sheared flows in a tokamak plasma can significantly reduce the ion thermal transport. In the presence of plasma fluctuations driven by the ion temperature gradient, the flows of energy and momentum parallel and perpendicular to the magnetic field are coupled with each other. This coupling manifests itself as significant off-diagonal coupling coefficients that give rise to new terms for anomalous transport. We derive from the gyrokinetic equation a set of velocity moment equations that describe the interaction among plasma turbulent fluctuations, the temperature gradient, the toroidal velocity shear, and the poloidal flow in a tokamak plasma. Four coupled equations for the amplitudes of the state variables radially extended over the transport region by toroidicity induced coupling are derived. The equations show bifurcations from the low confinement mode without sheared flows to high confinement mode with substantially reduced transport due to strong shear flows. Also discussed is the reduced version with three state variables. In the presence of sheared flows, the radially extended coupled toroidal modes driven by the ion temperature gradient disintegrate into smaller, less elongated vortices. Such a transition to smaller spatial correlation lengths changes the transport from Bohm-like to gyroBohm-like.

[a]Naka Fusion Research, JAERI, Japan

The properties of these equations are analyzed. The conditions for the improved confined regime are obtained as a function of the momentum-energy deposition rates and profiles. The appearance of a transport barrier is a consequence of the present theory.

I. INTRODUCTION

In modern auxiliary heated large tokamaks the instability driven by the ion temperature gradient such as the ion temperature gradient (ITG) mode and the η_i-mode[1-4] plays a central role in determining the anomalous heat transport across the magnetic flux surfaces via the ion energy channel. It has been experimentally[5,6] found that the ion temperature gradient is close to the marginal value of the instability. In a recent series of computational and theoretical investigations[7-9] we have, among others, shown that these modes are excited in a radially extended domain that encompasses many rational surfaces and many ion Larmor orbits due to the poloidal (angle) coupling arising from the toroidicity of the tokamak plasma. This new physical understanding of transport has arisen from the emergence of recent progress in high temperature and low collisional tokamaks that was accomplished with strong auxiliary heating and in sophisticated toroidal computational codes[7-9] that can look into collisionless collective dynamics.

Spurred partially by this understanding and further by the recent advances in strong drives of flows in hot tokamak plasmas,[10,11] the properties of plasma stability and confinement in the presence of such flows have become a primary research interest. Even though the neoclassical ion orbit loss mechanism has been suspected as the origin of the confinement transition property (the L-H transition) by numerous authors,[13-18] the recent discovery of the transition from the low confinement (L-mode) regime to higher regimes (such as the VH-mode)[19-21] deep in the interior portions of the hot plasma has stimulated theoretical investigations of the roles the plasma flow may be playing in the core transport, as such a transition in a core plasma is unlikely to be directly linked to the neoclassical transport physics alone. The recent discoveries[20,21] of a transport barrier in the interior plasma dramatically underscore this point.

Horton and his collaborators[22-27] have considered the effects of plasma flows and their spatial shear on the plasma transport. They treated the self-consistent interaction of the fluctuation and the flow shear through the turbulent momentum fluxes. These works on coupled energy-momentum transports are on the resistive interchange mode[25] and some on the ion temperature gradient (ITG).[22-27] The work in Ref. 25 and that of Diamond and his colleagues[19] have incorporated the plasma flow shear dynamics into simple transport models that show the possible reduction of fluctuations and subsequent reduction of heat transport at low collisionality.

We carried out toroidal particle simulations based on the TPC code[26] including an external electric field which produces a poloidal plasma flow. Shown in Fig. 1 is an illustration of the electrostatic potential contours for three separate runs with or without external flows. In Fig. 1(a) no external flow is applied, while in Figs. 1(b) and (c) external flows in the ion diamagnetic direction and the electron diamagnetic direction are applied respectively. The applied external radial electric field that produces the poloidal flow is $E_r(r) = \alpha r$, where r is the minor radial coordinate and α is a constant. The constant α is approximately equal to $-(v_p B_0/a)$ where v_p is the poloidal velocity, B_0 the toroidal field and the minor radius. Because of toroidal geometry $B_T = B_0/(1+r\cos\theta/R)$, the constant α gives rise to a sheared flow with $v'_\theta \cong v_p/R$ which shows that relatively weak shear produces a substantial change in the convection pattern. At the same time of development the level of electric fluctuations in Figs. 1(b) and (c) is much reduced over that in Fig. 1(a). In Fig. 1(a) the typical long streamers from the coherent ballooning mode and radially connected structures observed in toroidal particle simulation[7] and two-dimensional linear toroidal eigenvalue theory[27,28] are evident. In Fig. 1(b) the mode rotation and the flow direction are the same and the streamer structure is adjusted by the presence of flow shear in such a way as to undo some of the magnetic sheared potential streamers in the original eigenfunction of Fig. 1(a). On the other hand in Fig. 1(c) the external flow direction is opposite to the mode rotation direction.

The mode amplitude is much reduced and the radial correlation length is shortened. More detailed analysis of this numerical experiment will be given elsewhere.

In Sec. II we outline the derivation of transport equations that describe the temporal evolution of (i) the plasma fluctuations, (ii) the temperature gradient, and (iii) the two components of shear flows from the kinetic equation of the plasma and its moment equations. We condense the physics of these effects into four equations for the state space formed from quantities that measure these quantities over the transport region. We now call this the four-field model in Sec. III. As an application of these equations, we discuss the effect of the transition between the low and high confinement regimes in this section. In Sec. IV we discuss a reduced model with three field variables and obtain analytic properties of the solutions of different confinement regimes. In Sec. V we discuss the prospect for plasma control via shear plasma flow with externally imposed profile of poloidal and toroidal momentum inputs as well as energy deposition for quality improvements in reactor grade tokamak plasmas and we summarize and draw conclusions.

II. BASIC EQUATIONS

Dong and Horton[22] derive an expression for gyrokinetic perturbed distribution in the presence of shear flow [Eq. (6) in Ref. 22], which can be symbolically written through a linear, nonlocal operator $\mathcal{L}$ as

$$\delta f(\mathbf{x}, \mathbf{v}, t) = \mathcal{L}\left[f_M(x, v; n(x), T(x), \mathbf{B}(x), v_\parallel(x), v_E(x))\right] \phi(\mathbf{x}, t), \tag{1}$$

where $\phi(x)$ is the local radial (x) function of the electrical potential, f_M the equilibrium distribution, L_s, L_n, L_T are the radial lengths and $v_\parallel(x), v_E(x)$ are the shear flow parallel to and perpendicular to the magnetic field. The equilibrium distribution is constructed from the constant of the motion and the perturbation δf contains the toroidal collisionless trajectories. Coupling this equation with the quasineutrality condition, they derive the

eigenfunction equation for the potential [Eq. (23) in Ref. 22], which is of the form

$$\left[\frac{\partial^2}{\partial x^2} + Q(L_n, L_T, L_s, v'_\parallel, v'_E, \omega, k_y x)\right] \phi_{k_y}(x) = 0, \tag{2}$$

where $v'_\parallel$ and v'_E are $\partial v_\parallel(x)/\partial x$, and $\partial v_E/\partial x$, respectively, and ω is the complex eigenfrequency. The potential Q arises from expanding the orbits locally for $k_x^2\rho_i^2 \ll 1$. Dong and Horton also give the corresponding integral operator equation that applies for $k_x\rho_i$ of order unity. Both operators describe the shearing of the fluctuation by the mass flow shear in $v_E(x)$ and $v_\parallel(x)$. The eigenvalues derived from Eq. (1) have been used to benchmark those from toroidal particle[7] and gyrofluid codes.

In Ref. 9 Tajima *et al.* found several physical characteristics of the toroidal ITG instability evolution through toroidal computation. They are: (i) the development of radially extended potential streamers localized to the outside of the torus, (ii) more robust ion temperature gradient instability than the cylindrical counterpart, (iii) radially constant eigenfrequency over many rational surfaces, (iv) global temperature relaxation toward the marginal stability profile, and (v) radially increasing thermal conductivity χ_i. The theory constrains the thermal flux so that χ_i exponentially increases radially. The Bohm-like scaling may be inferred in connection with the radially extended mode structure, as the mode length $2\pi k_x^{-1}$ scales not as ρ_i, but involves macroscopic size L_T.[9,29] Based on these findings, we can conclude that the ITG instability is strong enough to force the temperature $T_0(x)$ to relax to a global function determined by a global constant L_T such that to the first approximation $T_0(x)$ as $T_0 e^{-x/L_T}$. Deviations from this exponential profile are rapidly washed away by the instabilities. The value of the relaxed L_T^{-1} is close to the critical value $L_{T_c}^{-1}$. Both experiment[5,6] and theory[9] show that the value is slightly above the marginal stability $L_T^{-1} > L_{T_c}^{-1}$. In the present theory the small difference away from the marginal stability $e - e_c \equiv a(L_T^{-1} - L_{T_c}^{-1}) \ll 1$ characterizes the level of turbulence in toroidal plasma and its associated transport, where a is the minor radius. Such a situation is not too far different[30] from the stellar temperature gradient of the

convectively unstable (convection zone, or sometimes called superadiabatic zone, according to the Schwarzschild condition[31]) plasma. In the convection zone the temperature gradient is slightly above critical so as to induce relatively weak convective turbulence that determines the transport of stellar energy flow due to the interior thermonuclear burn. It is surprising that nearly all types of stars in the main sequence maintain this feature.[30]

In Ref. 9 we developed a relaxation theory based on the reductive perturbative ordering in powers of W, which is akin to a quasilinear theory [see Eq. (7) in Ref. 9]. In this perturbation expression the lowest order thermal balance is given by

$$\frac{\partial T_0(x,t)}{\partial t} + \nabla \cdot \mathbf{q}(x,t,|\phi|^2) = 0, \tag{3}$$

where the heat flux $\mathbf{q}$ is a quadratic power of $\phi(x)$ found in Eq. (2). Based on this theory Tajima *et al.*[9] and Kishimoto *et al.*[32] have established a two-field model that describes the coupled evolution of turbulence and the associated deviation of the temperature gradient from the critical gradient. They were able to show the L-mode scaling and its confinement degradation due to high power heating. The main feature of the theory is based on the radially extended fluctuation structure.

In the present paper we extend this two-field model to include shear flow effects. The two equations in Ref. 9 are (i) the equation that describes the slow time scale evolution of ITG fluctuations, $|\phi|^2$ and (ii) the equation that describes the temperature gradient $e(t)$ evolution. The former equation is now generalized to include shear flows as well as neoclassical effects, following the Su *et al.* work[25] (with a slight simplification), as

$$\frac{\partial |\phi|^2}{\partial t} = \left[2\gamma(e-e_c) + c_1 F_{\|} - c_2 F_{\perp} - 2\gamma_n |\phi|^2\right] |\phi|^2, \tag{4}$$

where $\gamma(e-e_c)$ is the linear growth rate of the ITG instability, $e \equiv a/L_T$, $e_c \equiv a/L_{T_c}^{-1}$ critical temperature gradient, $F_{\|}$ and $F_{\perp}$ are the parallel and perpendicular shear flow energies and $\gamma_n |\phi|^2$ is the nonlinear stabilization of the instability. The temperature gradient equation

may be derived[32] from the second velocity moment equation of the kinetic equation

$$\tfrac{3}{2}\frac{\partial T}{\partial t} = \frac{1}{r}\frac{\partial}{\partial r} r\chi(|\phi|^2, L_T, \ldots)\frac{\partial T}{\partial r} + P/n, \tag{5}$$

where in Eq. (5) we assumed that the density profile is slowly varying in (r,t) compared with temperature profile. Here we freeze the density profile for simplicity and introduce auxiliary heating power density P. Then P/n is the heating rate per ion particle. Equation (5) determines the global temperature; however, by differentiating Eq. (5) with respect to r and dividing by T we can generate an equation for the gradient parameter $e(t) = a/L_T(t)$. Here T is the background temperature T_0 in Eq. (3) and Eq. (5) describes the slow (quasilinear) evolution in the relaxation theory.[32] We thus obtain

$$\frac{\partial e}{\partial t} = \frac{\partial}{\partial r}\frac{1}{r}\frac{\partial}{\partial r}\left(r\chi(|\phi|^2)T(r)\right) - \nu_{\rm nc}\, e + \frac{P(r)e}{nT(r)}, \tag{6}$$

where $\nu_{\rm nc} = 0.66\nu_{ii}/\epsilon^{3/2}(1+\nu_*)$ is the neoclassical collisional thermal relaxation rate with $\nu_* = \nu_{ii}qR/v_{th}\epsilon^{3/2}$.

An expression for the parallel flow shear $v'_\parallel$ is derived from the first velocity moment of the kinetic equation in the projection to the parallel direction. The general expression for the transport of parallel flow momentum is

$$\rho_m \frac{\partial v_\parallel}{\partial t} = -\rho_m \frac{\partial}{\partial x}(\pi_{\parallel x}) + P_p, \tag{7}$$

where $\rho_m = m_i n_i$ is the mass density, $\pi_{\parallel x}$ is the parallel-radial off-diagonal element of the Reynolds stress arising from the plasma fluctuations $|\phi|^2$, and P_p is the overall parallel momentum input power $P_p = m_i \int v_\parallel v^2 f d\mathbf{v}$. Following the work by Dong and Horton,[22] the radial derivative of the parallel flow velocity evolves from the fluctuations according to

$$\frac{\partial v'_\parallel}{\partial t} = \sqrt{\frac{\pi}{2}}\frac{cek_y|\phi|^2}{BT(r)}\frac{|\widehat{\omega}|^{7/2}}{s|\widehat{\omega}+K|^2}\left\{\frac{L_n}{4L_T^2}\frac{dv_\parallel}{dx} - \frac{L_n}{L_T}\frac{d^2v_\parallel}{dx^2}\right.$$
$$\left. + \frac{3L_n^3\gamma_0 K^2}{c_s^2 s|\widehat{\omega}+K|^4}\left(1 - \frac{\alpha}{c_s^2}u_\perp'^2\right)\frac{dv_\parallel}{dx}\left(\frac{d^2v_\parallel}{dx^2}\right)^2\right\} + \frac{1}{\rho_m}\frac{\partial}{\partial x}\left(\frac{P_p(r)}{nv_\parallel}\right), \tag{8}$$

where $v'_{\parallel} \equiv \partial v_{\parallel}/\partial x$, x is the local radial coordinate, $K \equiv \frac{T_i}{T_e}(1+\eta_i)$, $\widehat{\omega} = \omega/\omega_{*e}$, $u'_{\perp}$ is the poloidal shear flow, γ_0 is the linear growth rate of the mode and s is the magnetic shear parameter. The eigenvalues $\widehat{\omega}$ are given in Ref. 22 as a function of k_y for different values of $K, v'_{\parallel}, u'_{\perp}$ and s. Here we use Eq. (8) evaluated for a mean or typical value of these parameters.

The poloidal flow equation is similarly obtained from the off-diagonal Reynolds stress tensor due to electric fluctuations. According to Su *et al.*,[25] with a slight simplification we have

$$(1+2q^2)\frac{\partial u_{\perp}}{\partial t} = -\nu_{\rm nc} u_{\perp} - \frac{\partial}{\partial x}(\pi_{x\perp}), \tag{9}$$

where $\nu_{\rm nc} = \frac{e^{\rm nc}}{nm}\frac{B_t^2}{B_p^2 B_0^2}\left\langle\left(\frac{\mathbf{B}\cdot\nabla)B}{B}\right)^2\right\rangle$, q is the safety factor and $\pi_{x\perp}$ is the radial-perpendicular element of the Reynolds stress tensor, which is given as

$$\pi_{x\perp} = \frac{\sqrt{2\pi}\,|\phi|^2 c^2 k_y |\widehat{\omega}|^3 K}{B^2\rho_s s^{5/2}\gamma^{1/2}|\widehat{\omega}+K|^2}\left[1+\frac{\gamma\widehat{v}_{\parallel}''^2}{sK^2}\right]\widehat{v}_{\parallel}''. \tag{10}$$

Since $\widehat{C} = \sqrt{2\pi}(\widehat{\omega})^{5/2}K/s^{5/2}(\widehat{\omega}+K)^2 \sim$ const and $\widehat{A} = \gamma K^2/2s|\widehat{\omega}+K|^4 \lesssim 1 \sim$ const for the current model, $\partial\pi_{xy}/\partial x$ can be simplified and we obtain from Eq. (9)

$$\frac{\partial u_{\perp}}{\partial t} = |\phi|^2 \frac{c^2 k_y}{B^2\rho_s(r)}\frac{\sqrt{2\pi}\,|\widehat{\omega}|^{5/2}K}{|\widehat{\omega}+K|^2}\left\{\frac{L_n}{2c_s L_T}\frac{dv_{\parallel}}{dx}\right.$$

$$\left. + \left[1+\frac{\gamma^4\left(1-\frac{\alpha}{c_s^2}u_{\perp}'^2\right)}{sK^2c_s^2}\left(\frac{dv_{\parallel}}{dx}\right)^2\right]\frac{L_n}{c_s}\frac{d^2v_{\parallel}}{dx^2}\right\} - \nu_{\rm nc}u_{\perp}. \tag{11}$$

The stabilization effect of the ITG mode by the poloidal flow has been investigated by Dong and Horton,[22] who found that the reduction of the growth rate is a quadratic function of $u'_{\perp}$. The linear growth rate is now given as

$$\gamma = \gamma_0\left(1-\alpha u_{\perp}'^2\right) \tag{12}$$

where $u'_{\perp} \equiv (L_s/c_s)\partial u_{\perp}/\partial r$, and α is proportional to (L_s/c_s). For simpler hydrodynamic description the Waelbroeck *et al.*[27] obtain an exact analytic formula for γ that shows the same

features as Dong and Horton.[22] Earlier Tajima *et al.*[33] investigated the stabilizing influence of shear flows including the Kelvin-Helmholtz instability. The stabilizing mechanism is regarded as to reduce or eradicate the toroidicity-induced radial coupling due to the flow shear. If the toroidicity enhanced the radial correlation length (that is believed to lead the transition from the gyroBohm transport scaling in a cylindrical plasma to the Bohm scaling in a toroidal plasma[9]) beyond ρ_i and becomes a function of L_T in the absence of flow, the flow shear introduces a new mechanism to reduce the radial correlation length, which may bring the gyroBohm scaling back.

These dynamical equations, Eq. (4) with Eq. (12), Eq. (6), Eq. (8), and Eq. (11), constitute the basic equations that govern temporal evolution of the four transport variables, $|\phi|^2, \partial \ell n T_0/\partial r$, $\partial v_\parallel/\partial r$, and $u_\perp$ with two external control parameters $P(r)$ and $P_p(r)$. In the following we will normalize and simplify these equations and examine their properties and physical significance.

III. THE FOUR-FIELD MODEL

First, in order to simplify the coupled energy-momentum transport equations to describe the anomalous ion transport in the presence of flows based on the global relaxation phenomena shown in Refs. 9 and 32, we assert (i) that the temperature has been relaxed to the exponential profile $T_0(r) \propto e^{-r/L_T}$, where L_T is a global (or semiglobal) constant in the transport zone, (ii) that the eigenfrequency ω is a global(or semiglobal) constant for the radially extended modes, and (iii) that the amplitude of electric potential fluctuations (and its square $|\phi|^2$) is a global (or semiglobal) constant. Other physical quantities such as magnetic shear s can be a radial functions. However, in order to emphasize the radial profile of the ion temperature and the control parameters $P(r)$ and $P_p(r)$, we will suppress the radial dependence of s and other parameters in this work. In fact carefully monitored profiles of $P(r)$ and $P_p(r)$ may be crucial in controlling and/or improving the transport in the current

and future experiments and our future theoretical work need to incorporate these. When the external control parameters $P(r)$ and $P_p(r)$ have a strong r dependence, it may also influence the equilibrium radial distribution. However, in this work only the influence of the radial profile of control parameters manifests in the radial dependence of variables $|\phi|^2, e, v'_\parallel$, and $u_\perp$. Thus Eq. (8), for example, has a significant radial dependence only through $1/T(r)$ and $P_p(r)$ and thus the first term on the right-hand side of Eq. (8) has the coefficient proportional to e^{r/L_T} and other factors in the coefficients are radially independent. In Eqs. (6), (8), and (11) the explicit radial dependence through the background temperature profile is highlighted. Similar simplifications can be done on other basic equations.

A further simplification would be to drop even this radial dependence and replace the radial derivatives with appropriate inverse scale lengths and then averaged over the transport range Δ. In this section we adopt this further simplification. We cast these transport equations into a low order system of ordinary differential equations (ODE) model. With appropriate normalizations the basic equations in the ODE representation are now

$$\frac{\partial}{\partial \tau} W = \left[\tilde{\gamma}_{10}(\tilde{e} - \tilde{e}_c) - \tilde{\gamma}_n W - \tilde{c}_1 \tilde{u}_\perp^2\right] W, \tag{13}$$

$$\frac{\partial \tilde{e}}{\partial \tau} = -(\tilde{d} W \tilde{e} + \tilde{\nu}_2)\tilde{e} + \tilde{P}\tilde{e}, \tag{14}$$

$$\frac{\partial \tilde{u}_\perp}{\partial \tau} = -\tilde{\nu}_1 \tilde{u}_\perp + \tilde{c}_2 \tilde{v}'_\parallel \left[1 + \tilde{\gamma}_{02}(\tilde{e} - \tilde{e}_c)\tilde{v}'^2_\parallel (1 - \eta \tilde{u}_\perp^2)\right] W \tag{15}$$

$$\frac{\partial \tilde{v}'_\parallel}{\partial \tau} = -(\tilde{d}' W \tilde{v}'^2_\parallel + \tilde{\nu}_3)\tilde{v}'_\parallel + \tilde{P}' \tilde{v}'_\parallel, \tag{16}$$

where $\tilde{F}$ denotes normalized quantities derived from corresponding physical quantity F. In obtaining the dimensionless variables it is convenient to introduce a scale factor f. The normalizations are

$$\tau = f\nu t$$

$$W = \left(|\phi|^2 e^2 / T_e^2\right) L_n / \rho_s$$

$$\widetilde{v}'_{\|} = v'_{\|} a / c_s$$

$$\widetilde{u}_{\perp} = f u_{\perp} / c_s$$

$$\widetilde{P}' = nF v_{th} / f \nu n T$$

$$\widetilde{P} = P / f \nu n T$$

$$\widetilde{e} = -a \partial \ell n \, T_i / \partial r$$

$$\widetilde{\nu}_1 = \nu_{\text{nc pol}} / f \nu$$

$$\widetilde{\nu}_2 = \nu_{\text{nc}} / f \nu$$

$$\widetilde{\gamma}_{10} = \gamma_0 / f \nu \; (= \text{linear growth rate divided by } e - e_c)$$

$$\widetilde{\gamma}_n = (\gamma_{\text{nonlinear}} / f \nu) \rho_s / L_n$$

$$\widetilde{c}_1 = \gamma_0 / f^3 \nu$$

$$\widetilde{\gamma}_{20} = \gamma_0 L_n^2 / \omega_{*e} s K^2 a^2$$

$$\widetilde{c}_2 = \sqrt{2\pi} \, \frac{K}{s^{5/2}} \left(\frac{\omega}{\omega_{*e}} + K \right)^2 \left(\frac{\omega}{\omega_{*e}} \right)^{5/2} \left(\frac{L_y}{a} \right) \frac{\omega_*}{(f \nu)},$$

where

$$\overline{\omega}_* = k_y \rho_s c_s / L_n$$

Δ_v is the velocity shear spatial length

η is the nondimensional parameter (usually much less than unity),

$\widetilde{d} = \frac{1}{2} \, \frac{k_y \rho_i v_{thi} L_T}{2 \epsilon_T f \nu a^2} \, \frac{\rho_s}{L_n}$ (according to Refs. 9 and 32)

$$\tilde{d}' = \frac{3\sqrt{\pi/2}\,K^2}{s^2\left|\frac{\omega}{\omega_{*e}}+K\right|^6}\left(\frac{\omega}{\omega_{*e}}\right)^{1/2}\left(\frac{\omega^3\gamma_0}{\omega_{*e}^4}\right)\left(\frac{\bar{\omega}_*}{\omega_{*e}}\right)\left(\frac{L_n^3}{a^2\Delta_v}\right)\left(\frac{\rho_s}{L_n}\right)\left(\frac{\omega_{*e}}{f\nu}\right).$$

Equation (13) came from Eq. (4), Eq. (14) from Eq. (6), Eq. (15) from Eq. (11), and Eq. (16) arisen from Eq. (8). These four equations, or more accurately, the four-dimensional state model are a generalization of the two-dimensional state model that is defined by Eqs. (13) and (14) without the $u_\perp$ term in Eq. (13). Those equations reproduced the L-mode transport scaling.[32] In these normalizations we anticipate the variables and coefficients in Eqs. (13)–(16) are of the order unity for typical problems under study.

It is instructive to examine the physical meaning of each term in Eqs. (13)–(16). Equation (13) describes the temporal evolution of fluctuation energy W. The first term in the bracket is the linear growth rate, which is proportional to the difference of the temperature gradient away from the critical value $e - e_c$. The second term is the nonlinear (or quasi-linear) damping (saturation) due to the plasma turbulence. The last term is the stabilizing term due to the poloidal shear flow. In Eq. (14) the temperature gradient $\tilde{e} = -a\partial \ell n\, T_i/\partial r$ evolves according to the anomalous heat transport term $\tilde{d}W\,\tilde{e}$ (the first term on the right-hand side), which has arisen from $1/r\,\partial/\partial r(r\chi_i\,\partial T/\partial r)$, the neoclassical collision term (the second), and the heating term (the last term) that deposits energy in the plasma. This last power deposition term is the external control parameter (available to the experimenter).

The two components of momentum balance are given by Eqs. (15) and (16). In Eq. (15) the first term on the right-hand side is the neoclassical viscous damping and the rest is the anomalous off-diagonal Reynolds stress term which is driven by the presence of the toroidal flow shear. The toroidal shear flow is coupled with the poloidal flow through the plasma fluctuations. The coefficient $\tilde{c}_2$ is such a coupling coefficient. Equation (16) describes the time evolution of $v'_\parallel$, whose structure has a parallel to Eq. (14). The first term is the anomalous momentum transport, the second the neoclassical viscosity, and the last is the

input momentum deposition rate in the plasma. The control parameter P' can be zero even though the input energy deposition rate P is nonzero. This is because the net input momentum deposition can be balanced to zero by symmetric injection of opposing neutral beam injection (NBI) lines. Since the beam momentum deposition is sign dependent, P' can take both positive and negative signs. Several authors including those in Refs. 14-16 have used a similar set of equations to Eqs. (13)–(16) to explain the transition between L-mode and H-mode. Many of these theories[15–18] are solely based on neoclassical collisional effects and plasma instability and resultant turbulence play no role. Reference 19 began utilizing the effect of the plasma flow due to turbulence to explain the so-called VH mode[34] that develops deep inside of the hot plasma where the neoclassical effects cannot be important. Equation (13) has a Landau-Ginzburg type form, whose bifurcation properties the Itohs[15] have exploited for the explanation of the L-H transition in the edge plasma. However, in these works the model equations have been *a priori* set without attempt to derive them from more basic equations and fundamental simulations.

In the present work we started from the basic kinetic equations and took its moments. The moment equations are effectively closed by using a combination of neoclassical and turbulent transport terms. As in neoclassical theory we also recognize the different roles of the poloidal and toroidal components of the flow. Roughly speaking, the toroidal flow can be either destabilizing and stabilizing depending on the magnetic shear, the ratio B_p/B, and the strength of the shear flow gradient. Here we emphasize the former (stabilizing) possibility which dominates for strong toroidal flow gradients. On the other hand, the poloidal flow is strongly stabilizing. This is because radially extended streamers excited in a toroidal plasma[7–9] are torn apart by the presence of shear flows. The poloidal or perpendicular shear flow tends to simply destroy the radial structure.

In the present work we do not attribute solely the collisional effect to the cause of the L-H transition, but consider the effect of off-diagonal stress tensor due to the plasma fluctuations.

These off-diagonal elements can arise from the neoclassical effects as well, and, if the plasma is near the edge and of low temperature, we in fact expect the neoclassical off-diagonal term be of importance. In the present work, however, for simplicity we emphasize the off-diagonal Reynolds stress mediated by plasma fluctuations. In a more complete transport work, however, both neoclassical and anomalous effects in off-diagonal as well as explicit radial dependence have to be explored. Sugama and Horton worked on a problem of resistive ballooning mode keeping the neoclassical and anomalous transport rates on equal footing.[14]

In order to understand the physical properties of the set of equations (13)–(16), we look for the time-dependent steady-state solutions ($\partial/\partial t = 0$). From now on we drop the tildes and subscripts for simplicity. From Eqs. (13)–(16) the steady-state solution should satisfy

$$\gamma_0(e - e_c) - \gamma_n W - cu^2 = 0, \tag{17}$$

$$dWe + \nu - P = 0, \tag{18}$$

$$-\nu u + cv' \left[1 + \gamma_0(e - e_c)v'^2\right] W = 0, \tag{19}$$

$$d'Wv'^2 + \nu - P' = 0, \tag{20}$$

where we made $\tilde{c}_1 = \tilde{c}_2$, $\tilde{\gamma}_{01} = \tilde{\gamma}_{02}, \tilde{\nu}_1 = \tilde{\nu}_2 = \tilde{\nu}_3$ and wrote these constants simply as c, γ_0, and ν. A recent energy-momentum power balance analysis on TFTR by Ehnst[35] indicates that the ion heat diffusivity χ_i and toroidal momentum diffusivity χ_ϕ are of the same order. Furthermore, both are anomalous and both (exponentially) increase as a function of the minor radius. Thus we can set $d' = d$ in many of our investigations.

From Eqs. (18) and (20), we respectively obtain

$$e = \frac{P - \nu}{dW}, \tag{21}$$

and

$$v' = \pm \left(\frac{P' - \nu}{d'W}\right)^{1/2}. \tag{22}$$

From Eq. (19) we obtain

$$u = \pm\frac{c}{\nu}\left(\frac{P'-\nu}{d'W}\right)^{1/2}\left\{1+\gamma^0\left[\left(\frac{P-\nu}{dW}\right)-e_c\right]\left(\frac{P'-\nu}{d'W}\right)\right\}W, \tag{23}$$

where we substituted Eqs. (21) and (22) in e and v' in for for Eq. (19). By inserting expressions (21)–(23) in Eq. (17), we finally get a fourth-order polynomial equation for single variable W for the dimensionless turbulence level W

$$\begin{aligned}&\left(\gamma_n+\frac{\Delta P' c^3}{\nu^2}\right)W^4+\gamma_0 e_c\left(1-\frac{2c^3}{\nu^2}\Delta P'^2\right)W^3\\&+\gamma_0\left(\frac{2c^3}{\nu^2}\Delta P\Delta P'^2-\Delta P+\frac{c^3}{\nu^3}e_c^2\gamma_0\Delta P'^3\right)W^2\\&-2\frac{c^3}{\nu^2}e_c\gamma_0^2\Delta P\Delta P'^3W+\frac{c^3}{\nu^2}\gamma_0^2\Delta P^2\Delta P'^3=0,\end{aligned} \tag{24}$$

where $\Delta P \equiv (P-\nu)/d$ and $\Delta P' \equiv (P'-\nu)/d'$. Only positive, real roots for W of Eq. (24) are physically realizable. We are only interested in positive values of ΔP.

In order to derive analytic expressions for steady-state solutions for Eq. (24), we explore two limits. First let us discuss the weakly nonlinear regime where $W \ll 1$. In this case we keep only terms of the power of W^2, W, and W^0 and drop the terms of order W^4 and W^3. We have

$$\begin{aligned}&\left[\Delta P\left(-1+\frac{2c^3}{\nu^2}\Delta P'^2\right)+\frac{c^3}{\nu^2}e_c^2\gamma_0\Delta P'^3\right]W^2\\&-2\frac{c^3}{\nu^2}e_c\gamma_0\Delta P\Delta P'^3W+\frac{c^2}{\nu^2}\gamma_0\Delta P^2\Delta P'^3=0.\end{aligned} \tag{25}$$

Consider the case when

$$\Delta P > \frac{2c^3}{\nu^2}\Delta P\Delta P'^2+\frac{c^3}{\nu^2}e_c^2\gamma_0\Delta P'^3, \tag{26}$$

which may be said to be the case for high heating rate but low net momentum deposition rate. In this case there is only one positive, real root for W:

$$W \approx \frac{-\frac{c^3}{\nu^2}e_c\gamma_0\Delta P\Delta P'^3+\frac{c^3}{\nu^2}e_c\gamma_0\Delta P\Delta P'^3\sqrt{1+\frac{\nu^2}{c^3e_c^2\gamma_0\Delta P'^3}}\left[\Delta P\left(1-\frac{2c^3}{\nu^2}\Delta P'^2\right)-\frac{c^3}{\nu^2}e_c^2\gamma_0\Delta P'^2\right]}{\Delta P\left(1-\frac{2c^3}{\nu^2}\Delta P'^2\right)-\frac{c^3}{\nu^2}e_c\gamma_0\Delta P'^3}. \tag{27}$$

Equation (27) in the lower power limit takes the form

$$W \approx \frac{\Delta P}{e_c}, \tag{28}$$

while (27) takes the form in high power limit

$$W \approx \sqrt{\frac{\frac{c^3}{\nu^2}\gamma_0 \Delta P \Delta P'^3}{\left(1 - \frac{2c^3}{\nu^2}\Delta P'^2\right) - \frac{c^3}{\nu^2} e_c \gamma_0 \frac{\Delta P'^3}{\Delta P}}}. \tag{29}$$

The values of W in Eqs. (27) and (29) determine e, v', and u through Eqs. (21)–(23) and thus determine the effective thermal diffusivity. From the calculation of the thermal diffusivity we find that Eq. (28) is a typical L-mode scaling in the low input heating, where the fluctuation is linearly proportional to the input power.[32] Equation (29) has a hint of a typical L-mode scaling in the high power heating, although other complications are involved, where W is proportional to square root of the input power.[32]

Now consider the case where

$$\Delta P < \frac{2c^3}{\nu^2}\Delta P \Delta P'^2 + \frac{c^3}{\nu^2} e_c^2 \gamma_0 \Delta P'^3, \tag{30}$$

which means a high net momentum deposition rate measured here by $\Delta P'$. In this regime there are two real positive roots for W. They are

$$W_+ \approx \frac{2\frac{c^3}{\nu^2} e_c \gamma_0 \Delta P \Delta P'^3}{\Delta P(\frac{2c^3}{\nu^2}\Delta P'^2 - 1) + \frac{c^3}{\nu^2} e_c^2 \gamma_0 \Delta P'^3}, \tag{31}$$

and

$$\mathrm{W\_} \approx \begin{cases} \dfrac{\Delta P}{e_c} & \text{(low power limit)} \quad (32) \\ \dfrac{\frac{c^3}{\nu^2} e_c \gamma_0 \Delta P \Delta P'^3}{\Delta P(-1 + 2\frac{c^3}{\nu^2}\Delta P'^2) + \frac{c^3}{\nu^2} e_c \gamma_0 \Delta P'^3} & \text{(high power limit).} \quad (33) \end{cases}$$

Equation (32) applies when the second term in the radial of Eq. (27) is much less than unity, while Eq. (33) applied when it is of the order of unity.

The fluctuation level W bifurcates as shown in Fig. 2(a), as a function of the control parameter $\Delta P'$. When $\Delta P' > a \equiv \sqrt{\frac{\nu^2}{2c^3}}$, there exists no steady-state solution. Between $a > \Delta P' > b$, where b is the value of $\Delta P'$ which satisfies the condition

$$\Delta P - \frac{c^3}{\nu^2} e_c^2 \gamma_0 \Delta P'^3 - 2\frac{c^3}{\nu^2} \Delta P \Delta P'^2 = 0, \tag{34}$$

the boundary of Eqs. (26) and (30), there exist two steady-state solutions (the low and high confinement modes). Below $\Delta P' = b$, there is only one solution (the low mode). Thus when we raise the input momentum P' from below, or equivalently reducing the collisionality ν from above, the only possible equilibrium branch L is given a possibility to transit to the other branch (the high mode) when $\Delta P'$ exceeds the value b. This may be similar to the so-called L-H transition (or perhaps the VH mode transition) and could be an interpretation of the inducement of a transport barrier. The higher we increase $\Delta P'$, the smaller the gap between the low and high modes becomes and the easier the transition between the two. Eventually, at $\Delta P' = a$ they merge and $\Delta P' > a$ only temporary varying behaviors for W are permitted. In this regime oscillating solutions are possible, which may correspond to the ELMO signatures.[10,11] Correspondingly, the temperature gradient and the velocity shear also bifurcate as shown in Fig. 2(b) and (c). Figure 2(b) is based on $e = \Delta P/W$ (Eq. (21)) and Fig. 2(c) on $v'_{\|} = (\Delta P'/W)^{1/2}$ (Eq. (22)).

We can also analyze the opposite regime of a high turbulence W level. Here we retain only terms with W^4, W^3, and W^2 in Eq. (24), which leads to the form

$$\left(\gamma_n + \frac{\Delta P' c^3}{\nu^2}\right) W^4 + \gamma_0 e_c \left(1 - \frac{2c^3}{\nu^2} \Delta P'^2\right) W^3$$
$$+ \gamma_0 \left(\frac{2c^3}{\nu^2} \Delta P \Delta P'^2 - \Delta P + \frac{c^3}{\nu^2} e_c^2 \gamma_0 \Delta P'^3\right) W^2 = 0, \tag{35}$$

which is essentially a quadratic equation for nontrivial solutions for W ($W \neq 0$). We obtain

$$W = \frac{\gamma_0 e_c \left(\frac{2c^3}{\nu^2}\Delta P'^2 - 1\right) \pm \sqrt{\gamma_0^2 e_c^2 \left(\frac{2c^3}{\nu^2}\Delta P'^2 - 1\right)^2 - 4\left(\gamma_n + \frac{c^3 \Delta P}{\nu^2}\right)\left(\frac{2c^3}{\nu^2}\Delta P \Delta P'^2 - \Delta P + \frac{c^3 e_c^2}{\nu^2}\gamma_0 \Delta P'^3\right)\gamma_0}}{\left(2\gamma_n + \frac{\Delta P' c^3}{\nu^2}\right)}. \tag{36}$$

Case $\Delta P'^2 > \frac{\nu^2}{2c^3}$

This case of high momentum injection and low collisionality satisfies automatically the condition Eq. (30) and Eq. (36) gives two real positive roots, which are approximately

$$W_+ \approx \frac{\gamma_0 e_c \left(\frac{2c^3}{\nu^2}\Delta P'^2 - 1\right)}{\gamma_n + \frac{c^3}{\nu^2}\Delta P'}, \quad \text{(larger } W \text{ branch)} \tag{37}$$

$$W_- \approx \frac{\frac{c^3}{\nu^2}\Delta P'^2 (2\Delta P + e_c^2 \gamma_0 \Delta P') - \Delta P}{e_c \left(\frac{2c^3}{\nu^2}\Delta P'^2 - 1\right)}, \quad \text{(smaller } W \text{ branch)}. \tag{38}$$

Case $\Delta P'^2 < \frac{\nu^2}{2c^3}$

This case of low momentum injection and low collisionality satisfies Eq. (26) and allows only one real positive root, which is approximately in a low power regime

$$W_+ \approx \frac{\Delta P \left(1 - \frac{2c^3}{\nu^2}\Delta P'^2\right) - \frac{c^3 e_c^2}{\nu^2}\gamma_0 \Delta P'^3}{e_c \left(1 - \frac{2c^3}{\nu^2}\Delta P'^2\right)}, \tag{39}$$

and in high power regime

$$W_+ \approx \sqrt{\frac{\Delta P \gamma_0 \left(1 - \frac{2c^3}{\nu^2}\Delta P'^2\right) - \frac{c^3}{\nu^2} e_c^2 \gamma_0^2 \Delta P'^3}{\left(\gamma_n + \frac{c^3}{\nu^2}\Delta P'\right)}}. \tag{40}$$

Equation (39) is the low power L-mode-like and Eq. (40) is the saturated L-mode-like scalings. Condition (26) can be reached near the critical value $\Delta P'_c$, which is given by

$$\frac{c^3}{\nu^2} e_c^2 \gamma_0 \Delta P_c'^3 + \frac{2c^3}{\nu^2}\Delta P \Delta P_c'^2 - \Delta P = 0. \tag{41}$$

The overall behavior based on the high power analysis with the W^4, W^3, and W^2 terms is similar to that found from the low power analysis with the W^2, W, and W^0 terms in Eq. (24). For brevity of presentation we will not discuss this further.

We now investigate temporal evolution of the system of equations (13)–(16). In Fig. 3 we show an example of the time evolution of the four fields $W, e, v'_{\|}$, and $u_{\perp}$ and their projected phase space orbits $(W, e), (u_{\perp}, v'_{\|}), (W, u_{\perp})$, and $(e, v'_{\|})$ with a relatively small $\Delta P'$ value: the initial parameters (normalized) chosen are $\nu = 0.1, \Delta P = 0.15, \Delta P' = 0.15, d = d' = 1, c = 0.1, e_c = 0.1, \eta = 0.1$. In Fig. 4 we show a case with $\Delta P' = 1$ with the other parameters kept the same. In Fig. 5 we survey runs with various $\Delta P'$ ranging from 0.05 to 1.5 (other parameters are the same as in Fig. 3). Figure 6 surveys the ν scan from $\nu = 0.05$ to 1.5 with other parameters fixed at the canonical values.

IV. REDUCED THREE-FIELD MODEL: CONFINEMENT TRANSITION

In the previous section we derived four equations describing the four independent state variables, including the toroidal flow (shear) and poloidal flow. This is based on the realization that the toroidal flow shear can be either destabilizing or stabilizing depending on the detailed situation and parameters. Broadly speaking, the toroidal flow can enhance the overall centrifugal force that contributes to instability, while its shear could often shred the toroidally coupled mode structures, which contributes to stability. On the other hand, the poloidal flow (shear) is not destabilizing at the strengths reported and predicted. Certainly with enough shear, the shear flow instability may arise,[33] but this is not the regime of the tokamak experiments. The four state variable model in the previous section allows these competing physical effects to play their roles. On the other hand, it is rather cumbersome to analyze the four-dimensional state space. In this section, instead, we lump the shear flow energies into one variable, reducing the system to three equations. We follow the notation of Su *et al.*[25] for the shear flow energy F, which corresponds to the combination of $E_{bg,2}$ and $E_{fl,2}$ in Ref. 25. In this model we are simplifying the shear flow effect, perhaps a little overestimating its stabilizing influence. For this price we obtain a much more analytically

tractable model.

Let us go directly to the confinement regime where the confinement time τ_E (or W^{-1}) goes like $P^{-1/2}$, where e_c is not important. The balance of thermal energy (gradient) (e), wave energy (W), and shear flow energy (F) are then given as

$$\frac{dW}{d\tau} = [e - cF - \gamma_n W]\, W, \tag{42}$$

$$\frac{de}{d\tau} = -dWe + P, \tag{43}$$

$$\frac{dF}{d\tau} = [cW - \nu(e)]\, F + F^{1/2} P', \tag{44}$$

where we may allow the temperature dependence of the neoclassical collisionality ν. Here we simplified Eq. (13) to obtain Eq. (42) with $\gamma_{10} = 1$ and e_c is neglected. From Eq. (14) we neglected ν_2 to obtain Eq. (43) and simplified the power of e. In Eq. (15) we simplified the second term on the right-hand side and used Eq. (16) to get the shear flow coupling with the input momentum (a rough approximation as stated above) to obtain Eq. (44). Once we reduce Eqs. (14)–(16), the reduced set of three equations resemble those of Sugama and Horton.[14] We have, however, retained both external control parameters P (the energy deposition) and P' (the momentum deposition) as in the previous section. In the following we first discuss the physics (and confinement behavior) without P'. And then we go to the case with both P and P' present.

A. No Beam Momentum Injection ($P' = 0$)

We first identify fixed points of Eqs. (42)–(44); i.e. the steady solutions are given by

$$We = \frac{P}{d}, \tag{45}$$

$$e = cF + \gamma_n W, \tag{46}$$

and

$$F = 0 \qquad \text{or} \qquad cW = \nu. \tag{47}$$

The first case of Eq. (47) gives the fixed point

$$\text{(i)} \qquad F_0 = 0, \quad W_0^2 = \frac{P}{d\gamma_n}, \quad e_0 = \left(\frac{\gamma_n P}{d}\right)^{1/2}, \tag{48}$$

while the second case of Eq. (47) yields

$$\text{(ii)} \qquad W_1 = \frac{\nu}{c}; \qquad e_1 = \frac{Pc}{d\nu}; \quad cF_1 = e_1 - \gamma_n W_1 = \frac{c}{d\nu}(P - P_*), \tag{49}$$

where the subscript 0 or 1 refers to case (i) and (ii).

The condition to have case (ii) is from Eq. (49)

$$P > P_* = \frac{d\nu^2\gamma_n}{c^2}. \tag{50}$$

Now, we study the stability of the flow around these fixed points. In the neighborhood of these equilibrium states we linearize $\delta e \sim e^{\lambda t}, \delta W \sim e^{\lambda t}, \delta F \sim e^{\lambda t}$.

For (i) [Eq. (48)] $P < P^*$ ($F_0 = 0$) regime, we have

$$\lambda \begin{pmatrix} \delta e \\ \delta W \\ \delta F \end{pmatrix} = \begin{bmatrix} -dW_0 & -de_0 & 0 \\ W_0 & -\gamma_n W_0 & -c \\ 0 & 0 & cW_0 - \nu \end{bmatrix} \begin{bmatrix} \delta e \\ \delta W \\ \delta F \end{bmatrix}, \tag{51}$$

which yields $(\lambda + \nu - cW_0)\left[(\lambda + dW_0)(\lambda + \gamma_n W_0) + de_0 W_0\right] = 0$. There exist three modes: One is

$$\lambda_3 = -\nu + cW_0, \tag{52}$$

and the other two are

$$\lambda_\pm = \frac{-(d+\gamma_n)W_0 \pm \left[(d-\gamma_n)^2 W_0^2 - 4e_0 dW_0\right]^{1/2}}{2}, \tag{53}$$

where $W_0 = \left(\frac{P}{d\gamma_n}\right)^{1/2}$ and $e_0 W_0 = \frac{P}{d}$. The discriminant D of Eq. (53) is

$$D = (d-\gamma_n)^2 \frac{P}{d\gamma_n} - 4P = \left[\frac{(d/\gamma_n - 1)^2}{d/\gamma_n} - 4\right] P, \tag{54}$$

which vanishes at $d/\gamma_n = \dfrac{3 \pm \sqrt{5}}{2}$.

Thus, the discriminant is negative ($D < 0$) for $0.382 < d/\gamma_n < 2.62$, and the eigenvalues show oscillatory decay with

$$\lambda_{\pm} = - \pm i(P)^{1/2}\sqrt{X} - \frac{(d+\gamma_n)}{2}\left(\frac{P}{d\gamma_n}\right)^{1/2}, \tag{55}$$

where $X = 1 - (d-\gamma_n)^2/4d\gamma_n$. Now, the main point is that the δF-mode has the eigenvalue

$$\lambda_3 = cW_0 - \nu = c\left(\frac{P}{d\gamma_n}\right)^{1/2} - \nu, \tag{56}$$

and goes unstable at $P = P_* = \dfrac{\nu^2 d\gamma_n}{c^2}$, where we found the new equilibrium branch.

Now we examine the stability of the new branch (ii) [Eq. (49)] where

$$F_1 = \frac{P}{d\nu} - \frac{\gamma_n \nu}{c^2} = \frac{1}{d\nu}(P - P_*). \tag{57}$$

The stability problem is written by the perturbation matrix equation

$$\lambda \begin{pmatrix} \delta e \\ \delta W \\ \delta F \end{pmatrix} = \begin{bmatrix} -\dfrac{d\nu}{c} & -de_1 & 0 \\ \dfrac{\nu}{c} & -\dfrac{\gamma_n \nu}{c} & -\nu \\ -\dfrac{\partial \nu}{\partial e} F_1 & cF_1 & 0 \end{bmatrix} \begin{bmatrix} \delta e \\ \delta W \\ \delta F \end{bmatrix}, \tag{58}$$

which yields

$$\lambda\left[\left(\lambda + \frac{d\nu}{c}\right)\left(\lambda + \frac{\gamma_n \nu}{c}\right) + \frac{de_1 \nu}{c}\right] + \nu\left[\left(\lambda + \frac{d\nu}{c}\right) cF_1 + de_1 \frac{\partial \nu}{\partial e} F_1\right] = 0.$$

This can be cast into the form

$$\lambda^3 + A\lambda^2 + B\lambda + C = 0, \tag{59}$$

where

$$A = \frac{d\nu + \gamma_n \nu}{c} = (d + \gamma_n)(\nu/c), \tag{60}$$

$$B = \frac{d\nu^2\gamma_n}{c^2} + \frac{de_1\nu}{c} + c\nu F_1, \tag{61}$$

$$C = d\nu^2 F_1 + e_1 d\nu \frac{\partial \nu}{\partial e} F_1, \tag{62}$$

and

$$F_1 = \frac{(P - P_*)}{\nu d}. \tag{63}$$

For $|F_1| \ll 1$ we have

$$\lambda\left[\left(\lambda + \frac{d\nu}{c}\right)\left(\lambda + \frac{\gamma_n\nu}{c}\right) + P\right] + C \cong 0 \tag{64}$$

Since A and B are positive, the condition for the cubic Eq. (59) in λ to go unstable is that $C \propto (P - P_*)/\nu d$ be large enough that

$$C > AB, \tag{65}$$

or that $C < 0$. Here we are using that A and B are positive definite. Equation (65) is written as

$$\frac{(P - P_*)}{\nu d}(d\nu^2)\left(1 + \frac{e_1}{\nu}\frac{\partial \nu}{\partial e}\right) > \left[\frac{(d + \gamma_n)\nu}{c}\right]\left(\frac{d\nu}{c}\right)\left[e_1 + \frac{\gamma_n\nu}{c} + \frac{c^2 F_1}{d}\right]. \tag{66}$$

From Eq. (66) we see again the competition between the power (energy) injection on the left-hand side (when $[1 + d\ell n\,\nu/d\ell n\,e_1] > 0$) and the shear flow stabilization from F_1 on the right-hand side. We define $\tilde{P}$ (wiggle = onset of oscillation) above which the H-mode branch becomes oscillatory. When Eq. (66) is satisfied, we write for the excess $\delta C = C - AB$. As the power P increases above $\tilde{P}$ so that $\delta C > 0$, there is a Hopf bifurcation in the H-mode with a limit cycle occurring with the angular frequency $\omega_{\ell c} \simeq (B)^{1/2}$ with B from Eq. (61) and the amplitude of oscillation $\delta e, \delta W, \delta F$ proportional to $(\delta C)^{1/2}$ for small δC and saturating for larger δC. In the next subsection we show that the F_1-stabilization term on the right-hand side of Eq. (66) is enhanced by momentum injection P'.

The second type of instability from Eqs. (58)–(62) is a thermal instability when C goes negative. The confinement goes out of the H-mode state without oscillations with the slow exponential growth rate $\lambda = -(C/B) > 0$. This thermal instability occurs when the collisional damping decreases sufficiently rapidly with the temperature gradient e_1 such that

$$\left(1 + \frac{d\ell n \nu}{d\ell n\, e_1}\right) < 0. \tag{67}$$

Such a condition occurs when $\ell n(\nu) = (3/2)\ell n\, T_i + \ell n\, n$ is linked to the temperature gradient $e_1 = a/L_{T_1}$. Qualitatively, we expect that a steep gradient, large e_1, produces a large T_i/T_e. Quantitatively, we argue either (i) from $T_i(r+b) = T_i(\text{edge}) \exp\left[(a - r_{tb})/L_{T_i}\right]$ or (ii) from the marginal stability condition that $R/L_{T_i} > 0.2(1 + T_i/T_e) \simeq T_i/5T_e$ to conclude that $1 - \frac{3}{2}\, d\ell n\, T_i/d\ell n\, e_1 \approx 1 - \frac{3}{2} = -\frac{1}{2}$, and thus we obtain the weak exponential growth rate

$$\lambda_{us} = -\frac{C}{B} \simeq \frac{\nu d}{2c} \tag{68}$$

for the estimate of the thermally unstable H-mode that occurs when the collisionality decreases sufficiently rapidly with the increasing temperature gradient e_1.

In summary we see that for $P < P_*$ the effective thermal conductivity varies as $\chi_{\text{eff}} \propto (dP/\gamma_n)^{1/2}$ and that for $P > P_*$ the effective conductivity is $\chi_{\text{eff}} = (d\nu/c)$. For still higher injection power, and for certain conditions given by Eq. (66) we see that above the critical power $\tilde{P}$ the H-mode branch becomes oscillating. For $P > \tilde{P}$ then $W(t), F(t)$ and $e(t)$ oscillate about the H-fixed point values with the amplitude $\delta W, \delta F$ and δe increasing as $P - \tilde{P}$ and frequency of oscillation at first increasing with $P - \tilde{P}$ and then becomes almost independent of P.

B. Beam Momentum Injection ($P' \neq 0$)

For Eq. (44) with $P' \neq 0$ we have the fixed point

$$F_0 = \frac{(P')^2}{(\nu - cW)^2}, \tag{69}$$

and the new dynamical equation for perturbations to the flow δF given by

$$\delta\dot{F} = \left(-\frac{\partial\nu}{\partial e}\delta e + c\delta W\right) F_0 - \tfrac{1}{2}\frac{P'}{\sqrt{F_0}}\delta F. \tag{70}$$

The equilibrium now has three branches W_L, W_{H^+}, W_{H^-} and the coefficients A, B, C that determine the stability are given by

$$A^{\text{new}} = A^{\text{old}} + P'/2F_0^{1/2} \tag{71}$$

$$B^{\text{new}} = B^{\text{old}} + \frac{\nu}{c}(d+\gamma_n)(P'/2F_0^{1/2}) \tag{72}$$

$$C^{\text{new}} = C^{\text{old}} + \left(\frac{d\gamma_n\nu^2}{c^2} + P\right)\left(\frac{P'}{2F_0^{1/2}}\right). \tag{73}$$

The stability analysis is complicated, and the results depend on which branch of the equilibrium the system is on. Let us study the equilibrium now.

Three Equilibrium Branches for $P' \neq 0$

Using $e = P/dW$ and Eq. (68) for F_0 driven by P', we obtain the following condition of turbulent wave energy balance

$$\gamma(W) = \frac{P}{dW} - c\frac{P'}{(\nu - cW)^2} - \gamma_n W = 0. \tag{74}$$

It is convenient to rewrite condition (74) as

$$\left(W - \frac{\nu}{c}\right)^2\left(\frac{P}{dW} - \gamma_n W\right) = \frac{(P')^2}{c} \tag{75}$$

which clearly slows the coupling of the high-mode solution $W_H \equiv \nu/c$ to the low-mode solution $W_L = (P/\gamma_n d)^{1/2}$ by the perpendicular beam momentum input $P' \neq 0$.

For small P' we find the splitting of H-mode solution into two branches H^+ and H^- where H^+ (low W, high e) and H^- (high W, low e). The two H-mode turbulence levels are given by

$$W_{H^\pm} = W_H + W_{P'} \pm \left(W_{P'}^2 + W_H W_{P'}\right)^{1/2}, \tag{76}$$

where

$$W_{\rm H} = \frac{\nu}{c} \qquad \text{and} \qquad W_{P'} = \frac{d(P')^2}{cP}. \tag{77}$$

For $W_{P'} < W_{\rm H}$ or $d(P')^2 < P/\nu$ we have

$$W_{\rm H\pm} \cong W_{\rm H} \mp \sqrt{W_{\rm H} W_{P'}}, \tag{78}$$

with $W_{\rm H+}$ being the transport barrier solution.

For strong perpendicular beam heating where

$$d(P')^2 > P/\nu, \tag{79}$$

we get the very low turbulence level steady state

$$W_{\rm H+} \simeq \frac{W_L^2}{W_{P'}} = \frac{\nu^2 P}{cd(P')^2}, \tag{80}$$

and the relative high turbulence level and (probably unstable) branch $W_{\rm H-} \simeq 2W_{P'}$.

We may anticipate that the stability analysis of the $W_{\rm H+}$ may show the onset of oscillatory solutions for $P' > \tilde{P}$ (= the critical value) from A, B, C. This is the same as the case of the high $P(P' = 0)$ regime treated in Subsec. IV.B. A summary of this section may be given in Fig. 7 (Ref. 36).

V. SUMMARY

In a toroidal plasma (such as a tokamak) the toroidicity-induced coupling forces the modes that are originally localized near a rational surface to couple over a macroscopic radial extent. That is, without shear flow the radial correlation length develops a dependence on the size of the tokamak in addition to the microscopic scale lengths. As a result, for example, the ion temperature gradient (ITG) driven modes form radially extended streamers.[7–9] This global or semi-global mode structure[9,29,32] causes the plasma transport to manifest nonlocal signatures. Among these are the self-organized critical gradient behavior,[5,6,9,32] the

teleological transport as coined by Gentle,[37] and the Bohm-like scaling law for ion thermal diffusivity χ_i.[9,36] Because of this size dependence of the correlation length, we can construct transport model equations that govern these global (or semi-global) parameters such as the temperature gradient L_T^{-1} and fluctuation level W. Note that without such systems' constraint these parameters remain local parameters of a particular radial position, and we cannot avoid solving radial transport equations. Of course, typical transport codes do just this. In these radially dependent situations it is not feasible to construct and derive analytical tractable models and results, without introducing ad hoc assumptions. According to the self-organized critical gradient theory,[9,32] however, the field variables such as L_T^{-1} and W can now be regarded as (semi-global) state variables nearly independent of radial position r, instead of fields that are functions of r. Although we introduced a certain amount of approximations, such as a loose treatment of the changing value of the neoclassical collisionality, nonetheless, within the framework of the semi-global description we are able to start from the original gyrokinetic equations to systematically arrive at transport equations for these (semi)global transport variables.

Of particular importance in these transport equations are the effect of shear flows in a plasma, as regards to the recent advances in experimental research with strong external heating and flows.[10,11] The derived equations (13)–(16) are for the fluctuations $|\phi|^2$, the temperature gradient (normalized) e, the toroidal flow shear $v'_{\parallel}$, and the poloidal flow $u_{\perp}$. The external control parameters are not just the heating power deposition P but also the (toroidal) momentum deposition P_p (or P'). The main feature of the theory is that each transport variable is coupled with each other through the presence of plasma fluctuations W. The plasma fluctuations yield off-diagonal elements in the Reynolds stress tensor in the presence of plasma flows, since the flows break symmetry of the purely temperature (pressure) gradient driven instability.[14,22] In Sec. III we studied steady-state properties of Eqs. (13)–(16) and have seen the L-mode-like transport branch and the higher confinement

branch that is strongly influenced by the heating power deposition P and the momentum deposition P'. It is the momentum deposition P' that by and large reduces the transport decisively. Some of the temporal behaviors have been studied through numerical integration.

In order to enhance the analytical tractability and physical clarity, we isolated the effects of shear flows only to the stabilizing influence and neglected the distinction between the stabilizing part of the toroidal shear flow and the poloidal flows. In addition, we neglected the destabilizing part of the toroidal shear flow that occurs from the parallel Kelvin-Helmholtz modes. These simplifications appear to be well justified but are technically complex. Under additional simplifications we reduce the four state variable transport equations further to three state variable transport model Eqs. (42)–(44) for state variables of W, e, and the flow energy F. In these equations once again the external control parameters are not only the heating power deposition P, but also the momentum deposition P'. When the momentum deposition P' is zero (i.e. the balanced momentum injection) while the heating is on ($P \neq 0, P' = 0$), the description gives the (now familiar) L-mode-like transport branch and the "high confinement" branch that does not increase the transport even in the presence of increased heating power. The latter mode has signatures, some of which are common to the internal H-mode or the VH-mode. When the momentum deposition P' is no longer zero with the heating on as well ($P \neq 0, P' \neq 0$), there appears an additional bifurcation of confinement branches. The branch that has a lower level of fluctuations now shows a decrease in the fluctuations with increased momentum deposition. In a large momentum deposition regime the transport is severely suppressed [SSB (severely suppressed branch)] by the flow shear and the transport coefficient decreases as inversely proportional to $(P')^2$ [see Eq. (79)] for fixed energy deposition. This branch shows some of the signatures of the emergence of the transport barrier in the core plasma.[20] In both the JT60 and PBX-M systems the control of momentum injection appears critical to obtain the transport barrier.

The present theoretical approach and modeling may also be relevant to convectively

unstable reactor fluid dynamics and its heat transport as well as to the stellar convection zone transport.

Acknowledgments

The authors would like to thank our colleagues Drs. Y. Koide, M. Kikuchi, R. Yoshino, T. Fukuda, K. Gentle, and B. LeBlanc, on experimental discussion, and Drs. B. Coppi, F. Waelbroeck, F. Porcelli, M. Azumi, M. LeBrun, W. Dorland, and W. Tang for useful discussions and comments. We also thank Dr. K. Fujimura for discussion on fluid bifurcation and Dr. Shibahashi for discussions on stellar convection.

We appreciate the hospitality of Dr. H. Kishimoto and Prof. M. Date while two of the authors (TT,WH) stayed at JAERI. Dr. H. Maeda was instrumental in encouraging our work, whose untimely passing is a great loss to confinement research, and we would like to dedicate this paper to his memory.

The work was supported in part by the U.S. Dept. of Energy contract #DE-FG05-80ET-53088, and in part by JAERI Naka Fusion Establishment and Advanced Science Research Center. A portion of the work was carried out as a task of the Numerical Tokamak Project of the U.S. Dept. of Energy.

*also at Advanced Science Research Center, JAERI, Japan.

REFERENCES

[1]B. Coppi, M.N. Rosenbluth, and R.Z. Sagdeev, Phys. Fluids **10**, 582 (1967).

[2]W. Horton, D.I. Choi, and W.M. Tang, Phys. Fluids **24**, 1077 (1981).

[3]S.D. Scott, *et al.*, Phys. Fluids B **2**, 1300 (1990).

[4]for example, W. Horton, M. Wakatani, and A. Wootton, eds., *Ion Temperature Gradient-Driven Turbulent Transport* (AIP Conference Proceedings, No. 284, New York, 1994).

[5]T. Kurki-Suonio, R.J. Groebner, and K.H. Burrell, Nucl. Fusion **32**, 138 (1992).

[6]M. Kotschenreuther *et al.*, in *Plasma Physics and Controlled Nuclear Fusion Research, 1990*, Proc. 13th International Conf. (International Atomic Energy Agency, Vienna, 1991) Vol. II, p. 361.

[7]M. LeBrun, T. Tajima, M. Gray, G. Furnish, and W. Horton, Phys. Fluids B **5**, 752 (1993).

[8]S.E. Parker, W.W. Lee, and R.A. Santoro, Phys. Rev. Lett. **71**, 2042 (1993).

[9]T. Tajima, *et al.*, in *Ion Temperature Gradient-Driven Turbulent Transport* (AIP Conference Proceedings, No. 284, New York, 1994) p. 255.

[10]TFTR Group, to be published in *Plasma Physics and Controlled Nuclear Fusion Research, 1994*, Proc. 15th International Conf. (International Atomic Energy Agency, Vienna, 1995).

[11]JT60 Group, to be published in *Plasma Physics and Controlled Nuclear Fusion Research, 1994*, Proc. 15th International Conf. (International Atomic Energy Agency, Vienna, 1995).

[12]J.Y. Kim, Y. Kishimoto, W. Horton, and T. Tajima, Phys. Plasmas **1**, 927 (1994).

[13]ASDEX, Nucl. Fusion **29**, 1959 (1989).

[14]H. Sugama and W. Horton, Phys. Plasmas **1**, 345 (1994); and **1**, 2220 (1994).

[15]S. Itoh and K. Itoh, Phys. Rev. Lett. **60**, 2276 (1988).

[16]K.C. Shaing and E.C. Crume, Phys. Rev. Lett. **63**, 2369 (1989).

[17]P.N. Yushmanov, J.Q. Dong, W. Horton, X.N. Su, and S.I. Krasheninnikov, Phys. Plasmas **1**, 1905 (1994).

[18]H. Zohm, *et al.*, Phys. Rev. Lett. **72**, 222 (1994).

[19]P. Diamond, *et al.*, Phys. Rev. Lett. **72**, 2565 (1994).

[20]Y. Koide, *et al.*, Phys. Rev. Lett. **72**, 3662 (1994).

[21]B. LeBlanc, S. Batha, R. Bell, *et al.*, "Active core profile and transport modification, PPPL preprint (1994).

[22]J.Q. Dong and W. Horton, Phys. Fluids B **5**, 1581 (1993).

[23]W. Horton, J.Q. Dong, X.N. Su, and T. Tajima, J. Geophys. Res. **98**, 13377 (1993).

[24]J.Q. Dong, W. Horton, R.D. Bengtson, and G.X. Li, Phys. Plasmas **1**, 3250 (1994).

[25]X.N. Su, P. Yushmanov, J.Q. Dong, and W. Horton, Phys. Plasmas **1**, 1905 (1994).

[26]M.J. LeBrun and T. Tajima, submitted to J. Comput. Phys..

[27]F.L. Waelbroeck, *et al.*, Phys. Fluids B **4**, 2441 (1992); M. Artun and W.M. Tang, Phys. Fluids B **4**, 1102 (1992); M. Artun, J. Reynolds, and W.M. Tang, Phys. Fluids B **5**, 4072 (1993).

[28]W.M. Tang and G. Rewoldt, Phys. Fluids B **5**, 2451 (1994).

[29]F. Romanelli and F. Zonca, Phys. Fluids B **5**, 4081 (1993).

[30]E. Böhme-Vitense, *Introduction to Stellar Astrophysics* (Cambridge Univ. Press, Cambridge, 1989).

[31]M. Schwarzschild, *Structure and Evolution of the Stars* (Princeton Univ. Press, Princeton, 1958).

[32]Y. Kishimoto, *et al.*, to be published.

[33]T. Tajima, W. Horton, P.J. Morrison, J. Schutkekker, T. Kamimura, K. Mima, and Y. Abe, Phys. Fluids B **3** 938 (1991).

[34]GA and VH mode paper, in *Plasma Physics and Controlled Nuclear Fusion Research, 1994*, Proc. 15th International Conf. (International Atomic Energy Agency, Vienna, 1995).

[35]D. Ehnst, private communication (1994).

[36]Y. Kishimoto, *et al.* in *Plasma Physics and Controlled Nuclear Fusion Research, 1994*, Proc. 15th International Conf. (International Atomic Energy Agency, Vienna, 1995).

[37]K. Gentle, to be published in Phys. Plasmas.

FIGURE CAPTIONS

Fig. 1. The poloidal cross-section of equipotential contours for three different cases near saturation point of instability. (a) without external flow, (b) with external flow counterclockwise, (c) with external flow clockwise.

Fig. 2. The fluctuation level W, temperature gradient e, and the velocity shear $v'_{\|}$ as a function of the momentum input power $\Delta P'$ (definition in text). (a) W vs. $\Delta P'$, (b) e vs. $\Delta P'$, and (c) $v'_{\|}$ vs. $\Delta P'$. The point a is given by the condition $\Delta P' = a = (\nu^2/2c^3)^{1/2}$ and the point b is $\Delta P' = b$, where $\Delta P'$ satisfies the condition Eq. (34).

Fig. 3. The loci (orbits) of four state variables $W, e, v'_{\|}$, and $u_{\perp}$ as time goes by. $t\epsilon[0, 200]$. (a) e vs. W, (b) $u_{\perp}$ vs. W, (c) $v'_{\|}$ vs. $u_{\perp}$, and (d) $v'_{\|}$ vs. e for case $\nu = 0.1, \Delta P = 0.15, \Delta P' = 0.15, d = d' = 1, c = 0.1, \eta = 0.1, e_c = 0.1$.

Fig. 4. The loci (orbits) of four state variables $W, e, v'_{\|}$, and $u_{\perp}$ with time as a parameter. $t\epsilon[0, 200]$. (a) e vs. W, (b) $u_{\perp}$ vs. W, (c) $v'_{\|}$ vs. $u_{\perp}$, and (d) $v'_{\|}$ vs. e for case $\nu = 0.1, \Delta P = 0.15, \Delta P' = 1, d = d' = 1, c = 0.1$.

Fig. 5. Survey of parameter $\Delta P'$ from 0.05 to 1.5. (a) W vs. $\Delta P'$, (b) e vs. $\Delta P'$, (c) $u_{\|}$ vs. $\Delta P'$, and (d) $v'_{\|}$ vs. $\Delta P'$.

Fig. 6. Survey of parameters ν from 0.05 to 1.5. (a) W vs. ν, (b) e vs. ν, (c) $u_{\perp}$ vs. ν, and (d) $v'_{\|}$ vs. ν. ($\Delta P = 0.15$, $\Delta P' = 0.75$).

Fig. 7. Dependence of shear flow, temperature gradient, and plasma fluctuations (F, e, W) as a function of power deposition P and momentum deposition P'.

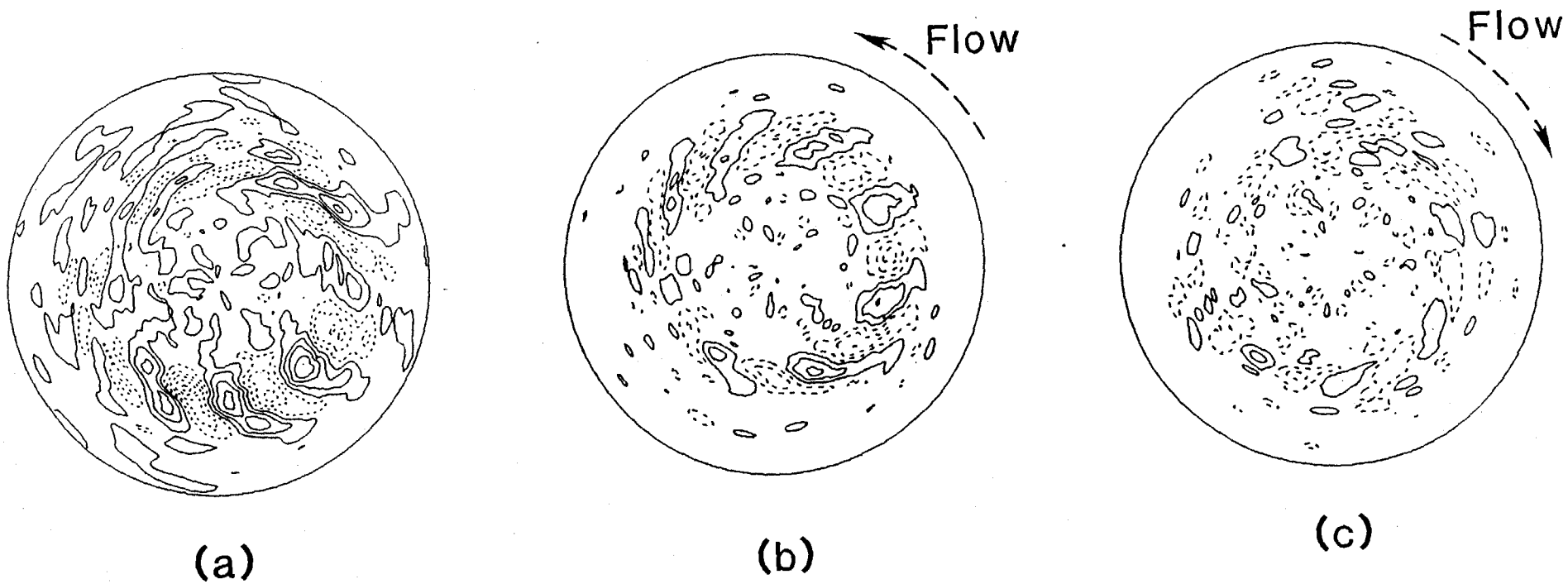

Figure 1

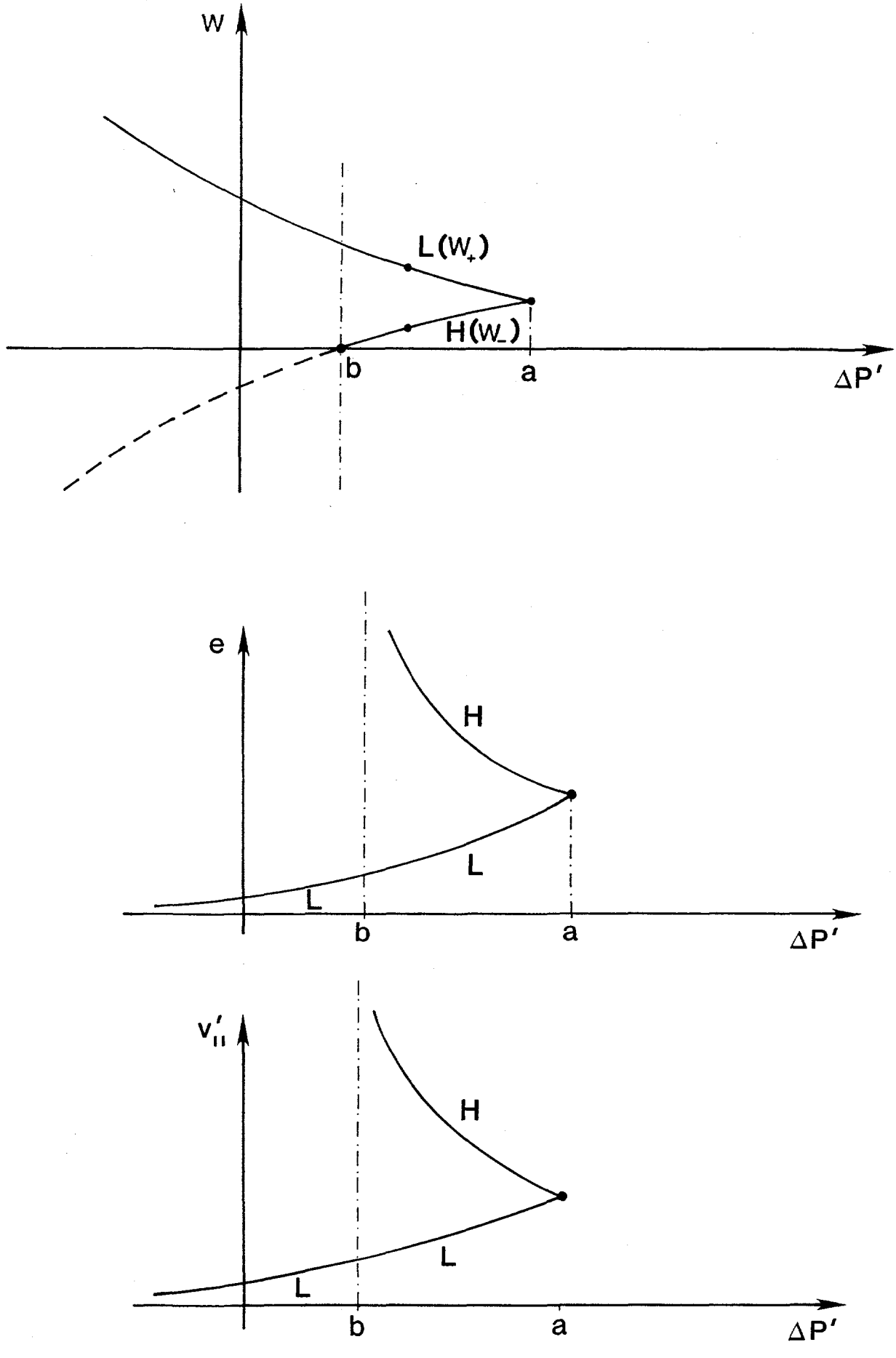

Figure 2

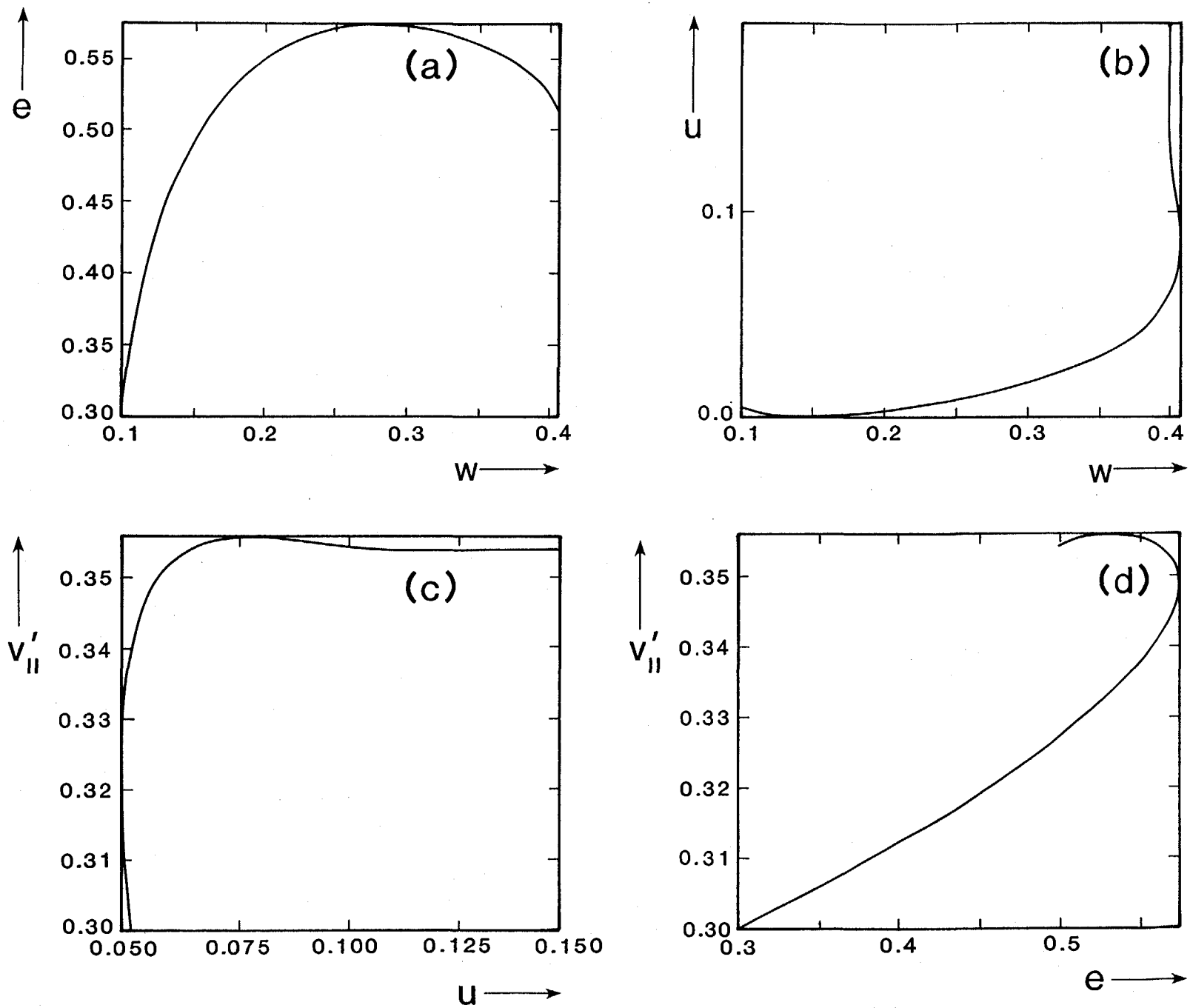
(a)
e
0.55
0.50
0.45
0.40
0.35
0.30
0.1
0.2
0.3
0.4
w
(b)
u
0.1
0.0
0.1
0.2
0.3
0.4
w
(c)
v_{II}'
0.35
0.34
0.33
0.32
0.31
0.30
0.050
0.075
0.100
0.125
0.150
u
(d)
v_{II}'
0.35
0.34
0.33
0.32
0.31
0.30
0.3
0.4
0.5
e

Figure 3

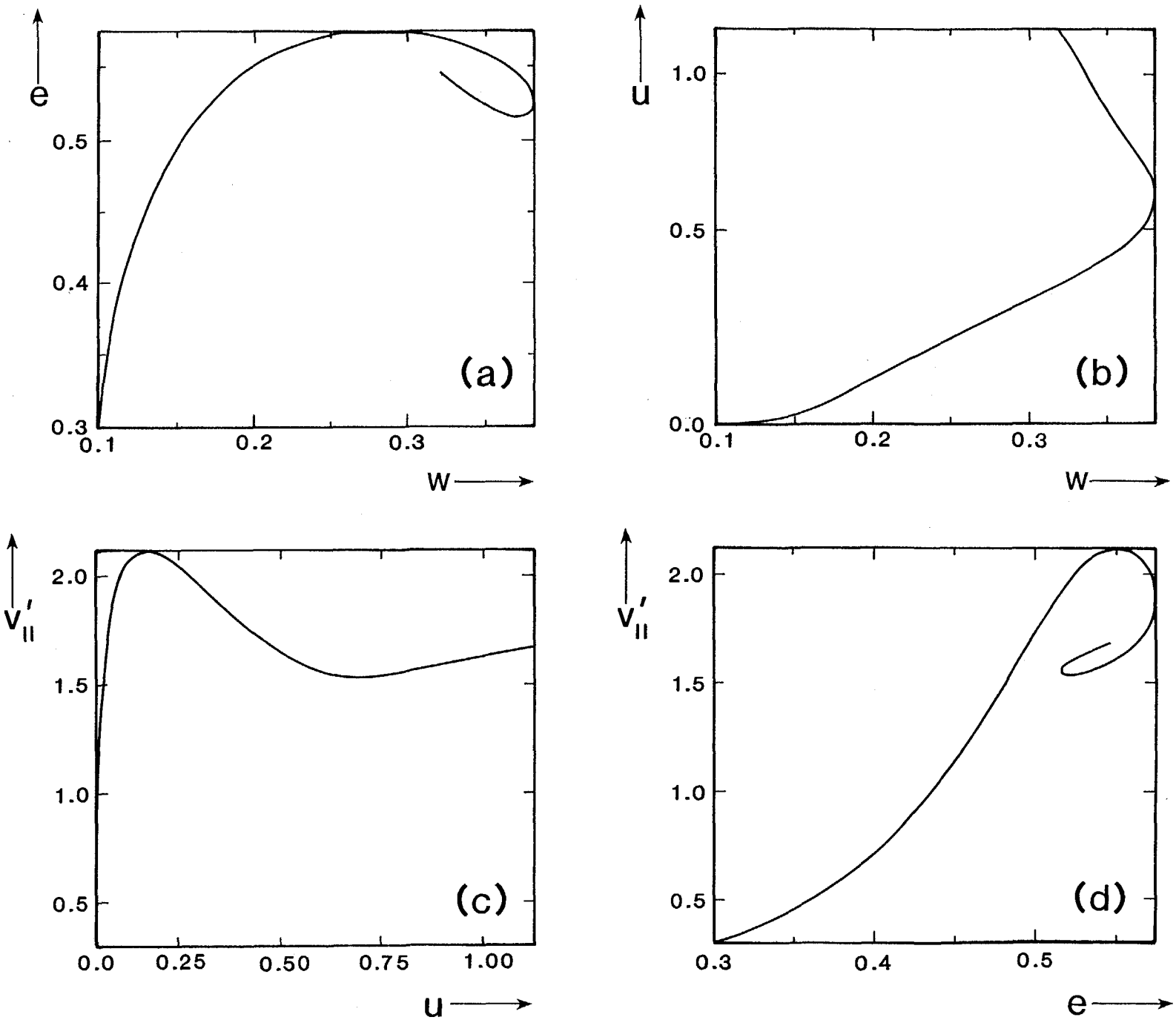
e
0.5
0.4
0.3
0.1
0.2
0.3
w
(a)
u
1.0
0.5
0.0
0.1
0.2
0.3
w
(b)
v_{II}'
2.0
1.5
1.0
0.5
0.0
0.25
0.50
0.75
1.00
u
(c)
v_{II}'
2.0
1.5
1.0
0.5
0.3
0.4
0.5
e
(d)

Figure 4

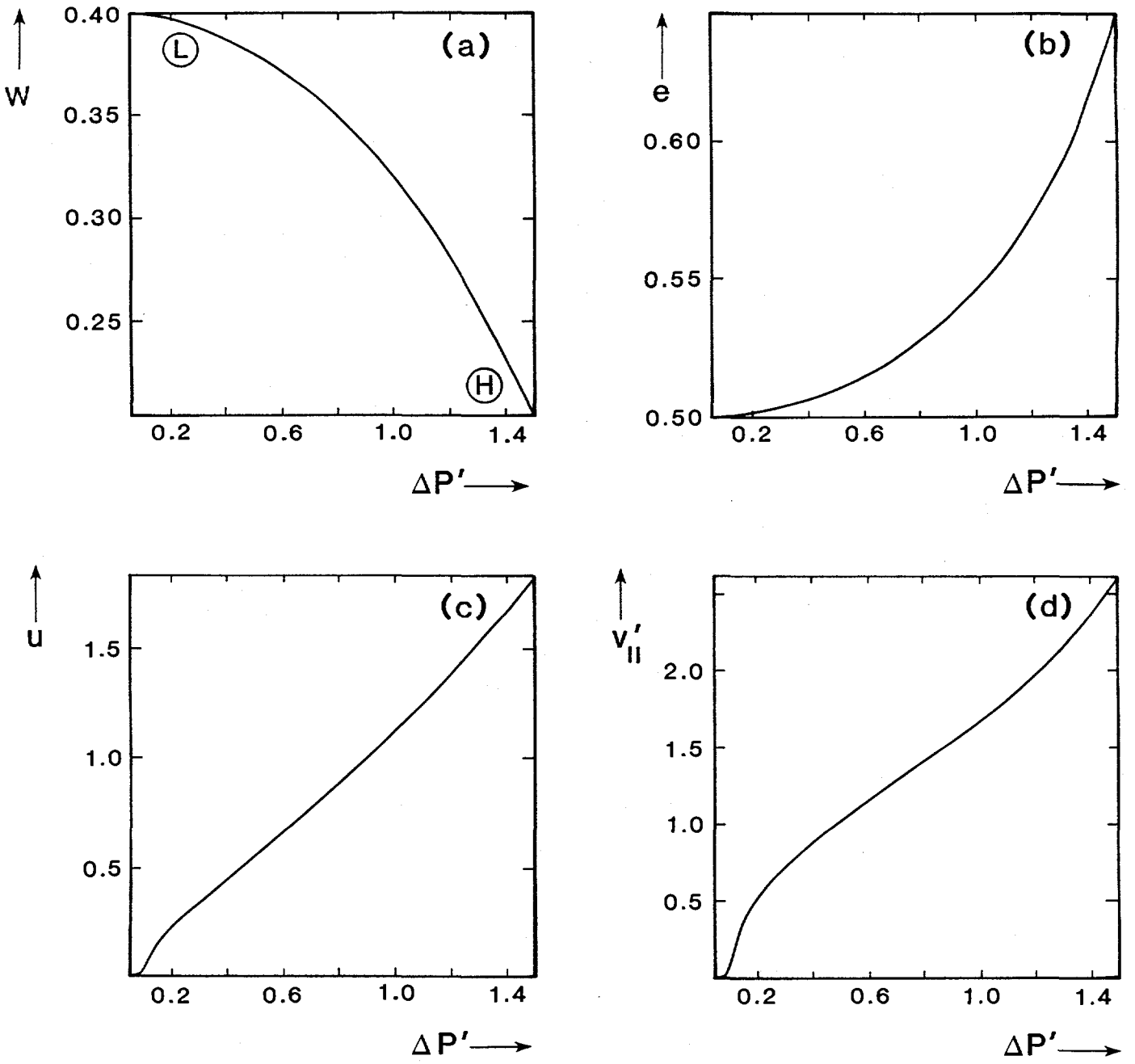
W
0.40
0.35
0.30
0.25
(a)
L
H
0.2
0.6
1.0
1.4
ΔP′
e
0.60
0.55
0.50
(b)
u
1.5
1.0
0.5
(c)
v_{II}'
2.0
1.5
1.0
0.5
(d)

Figure 5

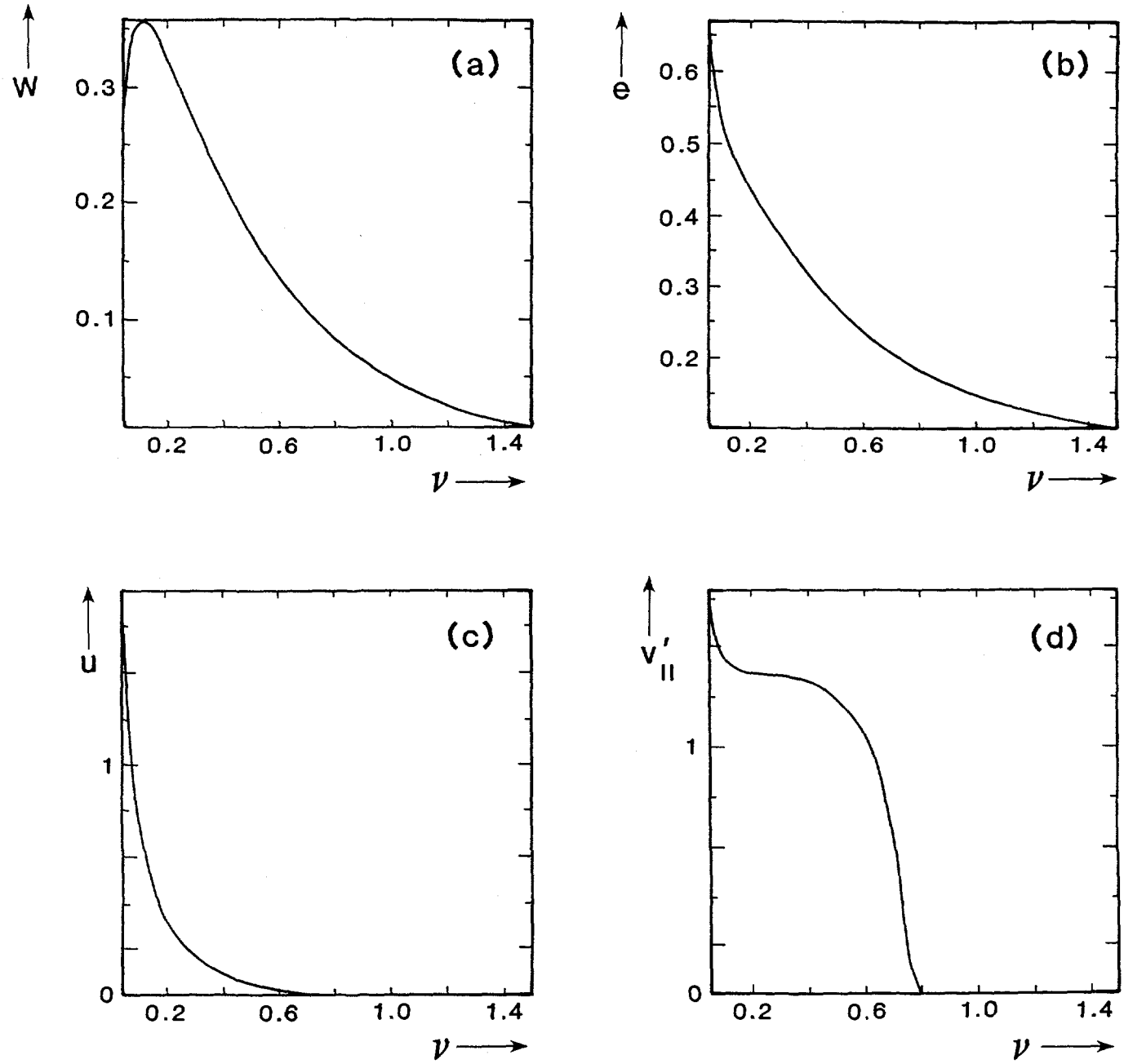
W
0.3
0.2
0.1
(a)
0.2
0.6
1.0
1.4
ν
e
0.6
0.5
0.4
0.3
0.2
(b)
0.2
0.6
1.0
1.4
ν
u
1
0
(c)
0.2
0.6
1.0
1.4
ν
V'II
1
0
(d)
0.2
0.6
1.0
1.4
ν

Figure 6

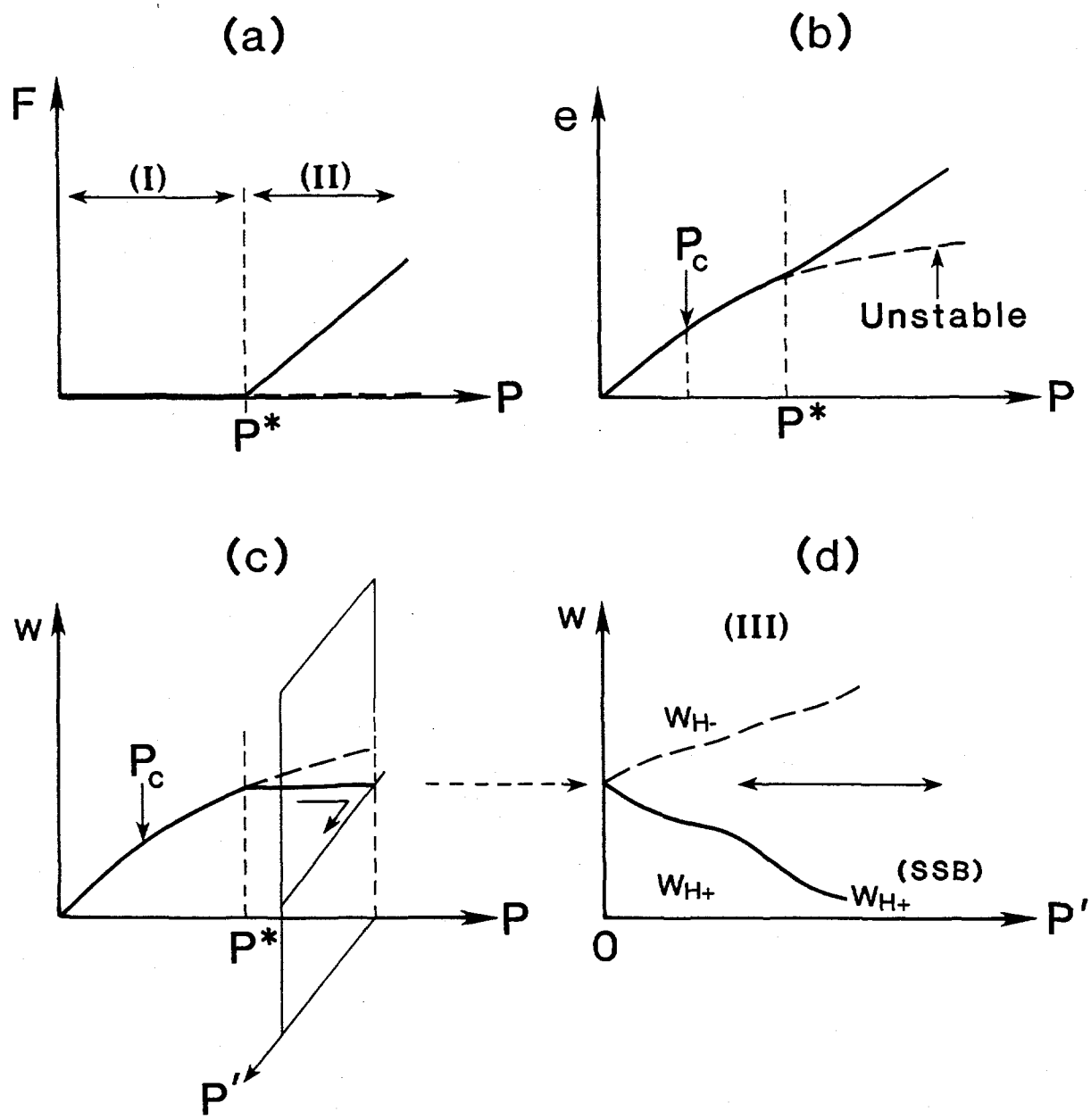

Figure 7